ELECTRONIC SUPPORTING INFORMATION (ESI)

Ag-Pd alloy supported on amine-functionalized UiO-66 as an efficient synergetic catalyst for dehydrogenation of formic acid at room temperature

Shu-Tao Gao, Weihua Liu, Cheng Feng*, Ning-Zhao Shang, Chun Wang*

$$x_a = \frac{P_{atm} V_{H_2} / RT}{n_{FA}} \qquad \text{Equation S1}$$

Where x_a is conversion, P_{atm} is the atmospheric pressure, V_{H_2} is the final generated volume of H_2, R is the universal gas constant, T is room temperature (298K), and n_{FA} is the mole number of FA.

$$TOF = \frac{P_{atm} V_{H_2} / RT}{n_{Ag+Pd} t} \qquad \text{Equation S2}$$

Where TOF is turnover frequency at a certain conversion of FA to H_2, V_{H_2} is the generated volume of H_2, n_{Ag+Pd} is the mole number of the Ag and Pd, and t is the reaction time.

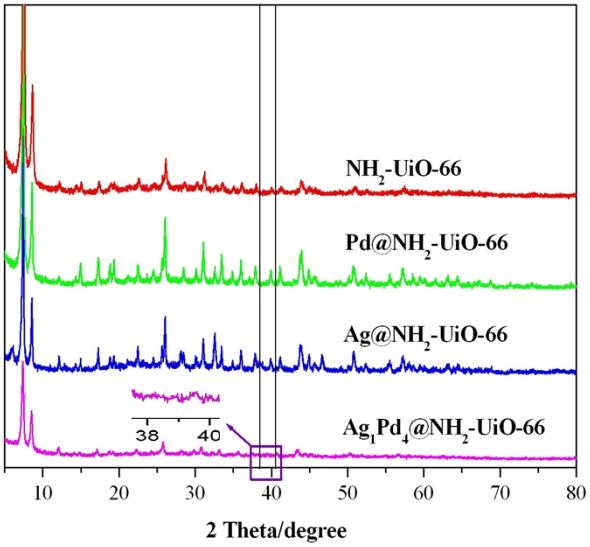

Figure S1 Powder X-ray diffraction patterns for NH_2-UiO-66, Pd@NH_2-UiO-66(5 wt%), Ag@NH_2-UiO-66(5 wt%), Ag_1Pd_4@NH_2-UiO-66(5 wt%).

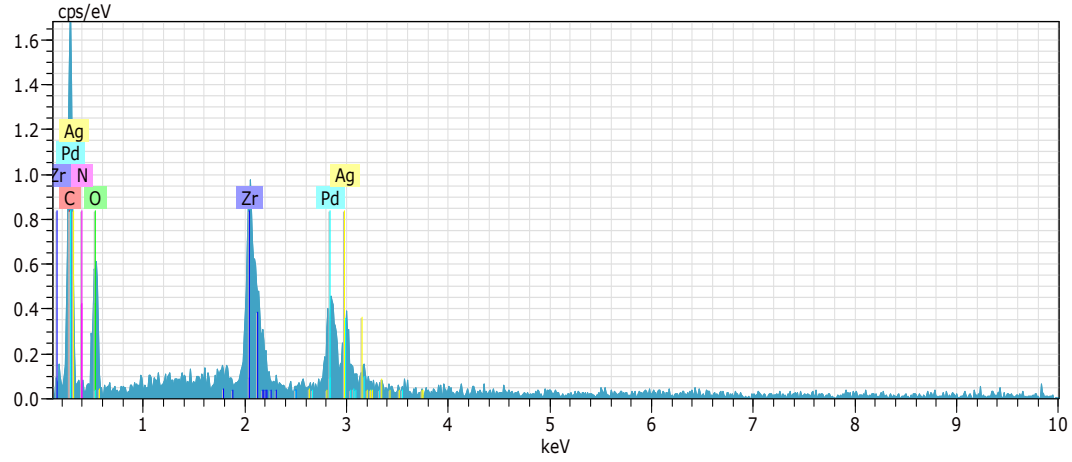

Figure S2 Energy-dispersive X-ray (EDX) spectrum of Ag_1Pd_4@NH_2-UiO-66.

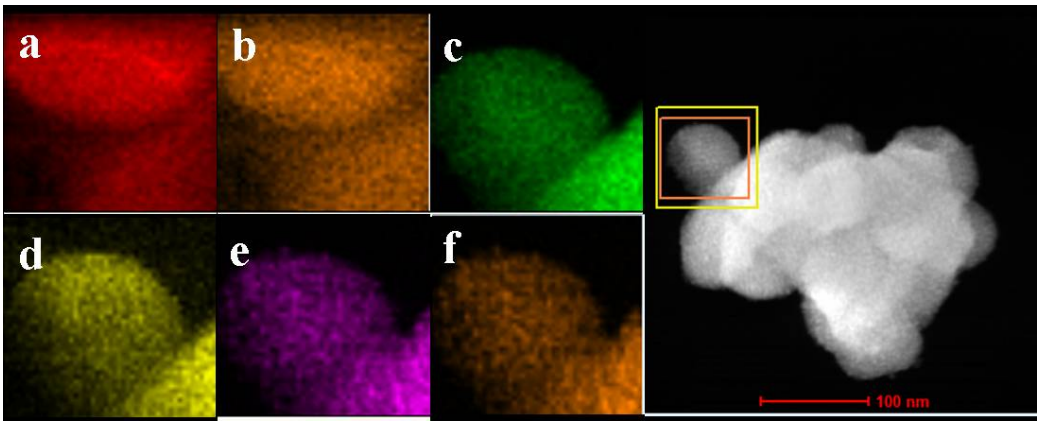

Figure S3 The corresponding elemental mapping for (a) C, (b) N, (c) Zr, (d) O, (e) Pd and (f) Ag elements and HAADF-STEM image of (g) Ag_1Pd_4@NH_2-UiO-66.

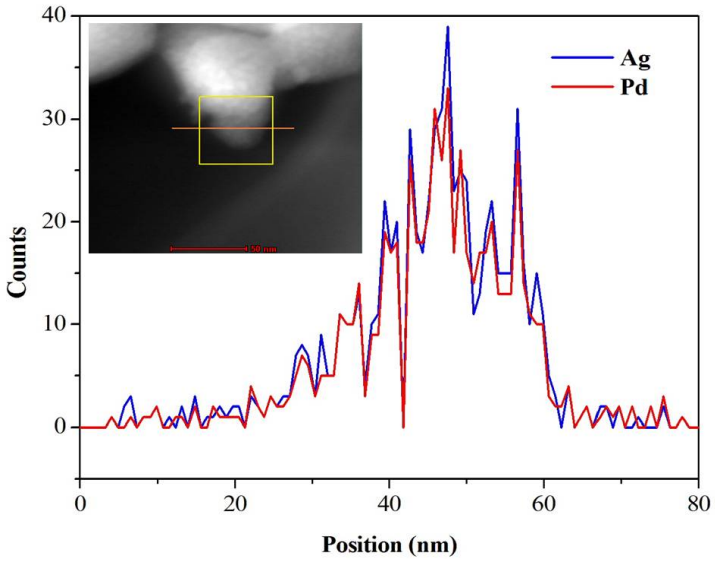

Figure S4 STEM-EDS line-scan EDS spectra of Ag_1Pd_4@NH_2-UiO-66.

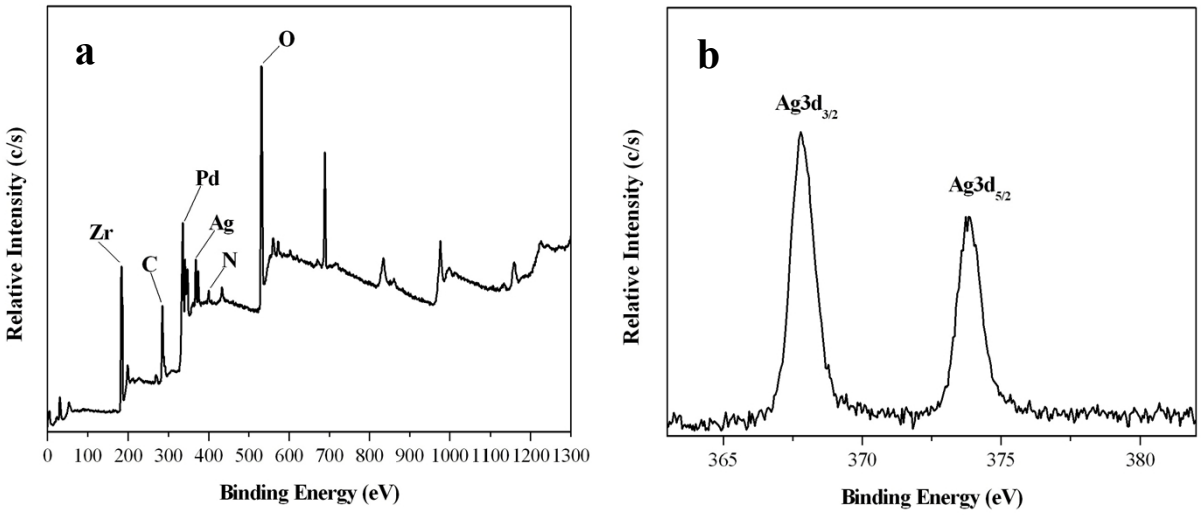

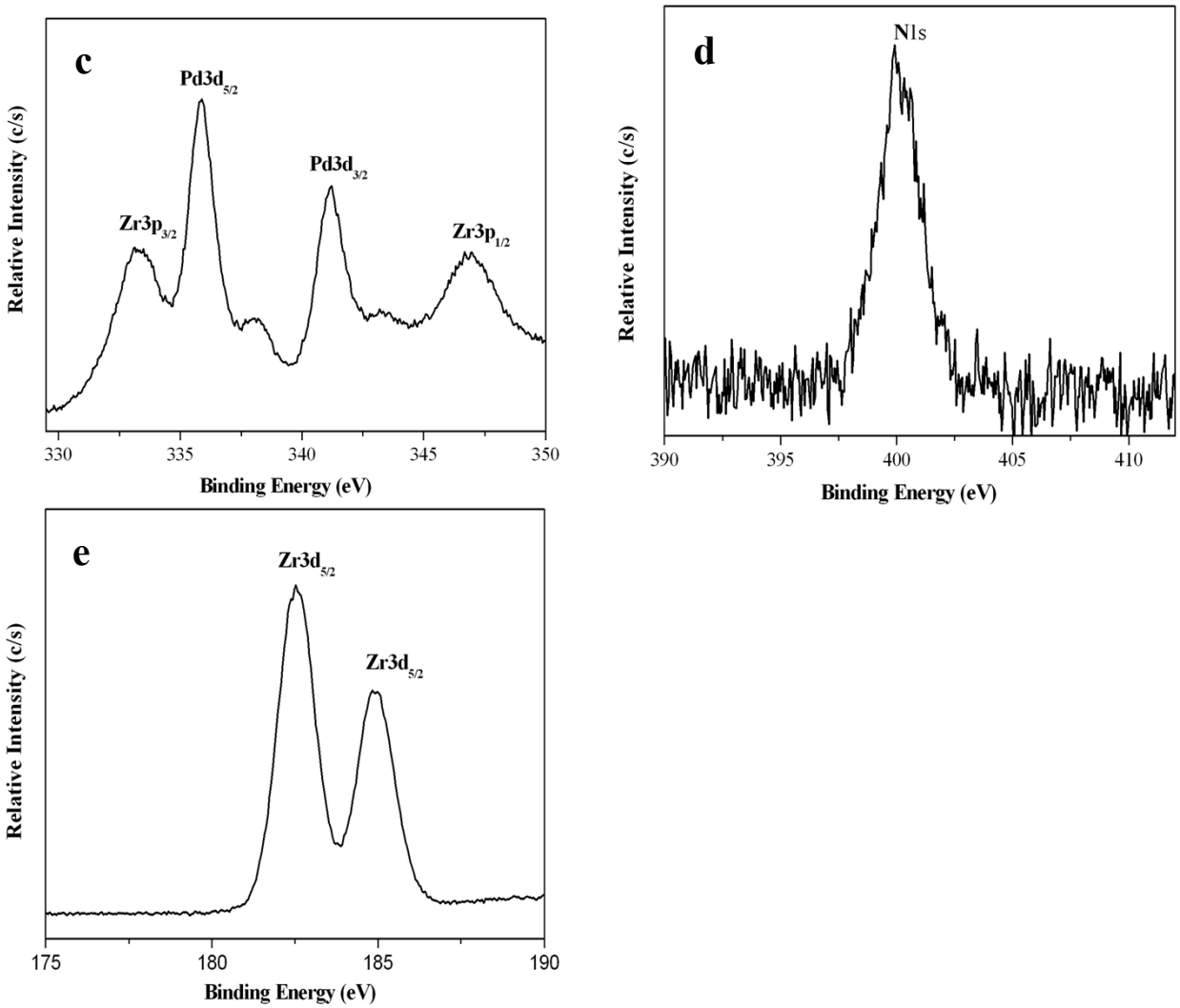

Figure S5 XPS patterns of Ag_1Pd_4@NH_2-UiO-66.

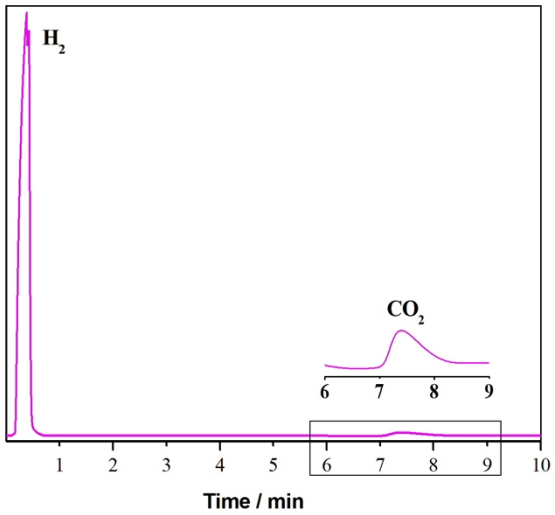

Figure S6 GC spectrum using TCD for the evolved gas from aqueous FA solution (1.25 M, 1.0 mL) over Ag_1Pd_4@NH_2-UiO-66 composite at 80 °C (n_{metal} / n_{FA} = 7.5×10^{-3})

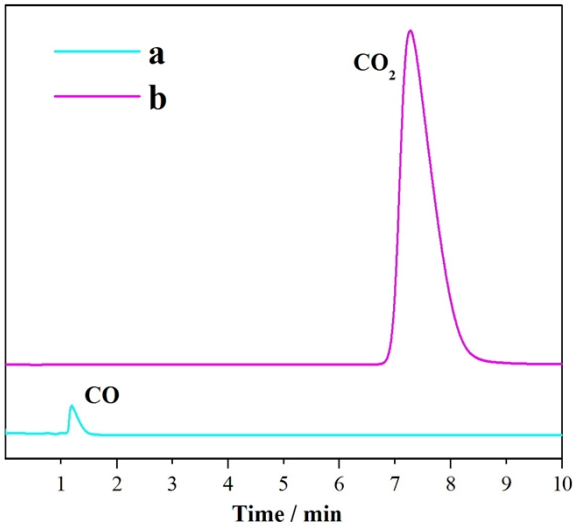

Figure S7 GC spectrum using FID-Methanator for the (a) commercial pure CO, and (b) evolved gas from FA aqueous solution (1.25 M, 1.0 mL) over Ag_1Pd_4@NH_2-UiO-66 composite at 80 °C (n_{metal} / n_{FA} = 7.5×10^{-3}).

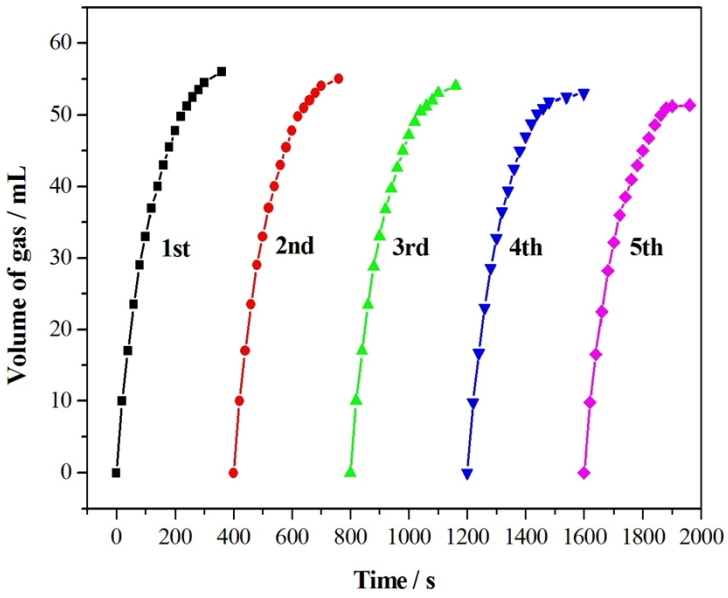

Figure S8 Stability test on the Ag_1Pd_4@NH_2-UiO-66 catalyst in the dehydrogenation of 0.42M FA aqueous solution at 80 °C